ELSEVIER

Geomorphology 40 (2001) 21–35

GEOMORPHOLOGY

www.elsevier.com/locate/geomorph

Natural and human-induced landsliding in the Garhwal Himalaya of northern India

Patrick L. Barnard [a], Lewis A. Owen [a,*], Milap C. Sharma [b], Robert C. Finkel [a,c]

[a] *Department of Earth Sciences, University of California, Riverside, CA 92521-0423, USA*
[b] *Centre for the Study of Regional Development, Jawaharlal Nehru University, New Delhi 110 067, India*
[c] *Center for Accelerator Mass Spectrometry, Lawrence Livermore National Laboratory, Livermore, CA 94550, USA*

Received 7 July 2000; received in revised form 9 January 2001; accepted 13 January 2001

Abstract

After the March 28, 1999, Garhwal earthquake, 338 active landslides, including 56 earthquake-induced landslides, were mapped in a 226-km^2-study area in the Garhwal Himalaya, northern India. These landslides mainly comprised shallow failures in regolith and highly weathered bedrock involving avalanches, slides, and flows. The total volume of active landslide debris in the region was estimated to be $\sim$1.3 million m^3 including 0.02 million m^3 ($<$2% of the total volume) moved during and within a few days of the earthquake. The denudation produced by the active landsliding within the study area is equivalent to a maximum landscape lowering of $\sim$5.7 mm. If active landsliding persists for a duration of between $\sim$1 and 10 years, then denudation due to landsliding is in the order of $\sim$0.6–6 mm a^{-1}. Approximately, two-thirds of the landslides in this region were initiated or accelerated by human activity, mostly by the removal of slope toes at road cuts, suggesting that human activity is accelerating denudation in this region. Three ancient catastrophic landslides, each involving $>$1 million m^3 of debris, were identified and two were dated to the early–middle Holocene using cosmogenic radionuclide ^{10}Be and ^{26}Al. Cosmogenic radionuclide ^{10}Be and ^{26}Al were also used to date strath terraces along the Alaknanda River in lower Garhwal Himalaya to provide an estimate of $\sim$4 mm a^{-1} for the rate of regional denudation throughout the Holocene. Natural landsliding, therefore, contributes $\sim$5–50% of the overall denudation in this region and is important as a formative process in shaping the landscape.

Keywords: Himalayas; Landslide; Cosmogenic dating; Fluvial incision; Denudation

1. Introduction

The role of landsliding in the denudation of Himalayan landscapes has been emphasized by many workers (Brunsden and Jones, 1984; Owen, 1991; Owen et al., 1995, 1996; Burbank et al., 1996; Hewitt, 1998; Shroder, 1998), yet there are few studies that quantify its importance. In the Himalaya, landsliding involves a variety and combination of processes, including falls, topples, avalanches, slides, and flows (Brunsden et al., 1981; Owen, 1991; Gerrard, 1994; Shroder and Bishop, 1998). Rapid tectonic uplift and the intense fluvial and

* Corresponding author. Tel.: +1-909-787-3106; fax: +1-909-787-3106.
E-mail address: Lewis.Owen@ucr.edu (L.A. Owen).

0169-555X/01/$ - see front matter
PII: S0169-555X(01)00035-6

glacial incision produces long steep slopes that are prone to failure. Failures in the Himalaya are commonly due to undercutting of slopes by fluvial erosion, shaking during earthquakes, and in the monsoon-influenced areas by the heavy rainfall leading to saturation and erosion of slopes (Brunsden et al., 1981; Owen, 1991; Owen et al., 1995, 1996). In recent decades, landsliding may have increased in many regions due to human activity, such as highway construction, deforestation, terracing, and agricultural activities. However, changes in the magnitude and frequency of landsliding due to human activity are widely debated (Ives and Messerli, 1989).

In this study, we will examine natural and human-induced landslides in a study area in the Garhwal Himalaya of northern India. This region was chosen because at 19:05 (GMT) on March 28, 1999, a magnitude 6.6 (M_s) earthquake shook the Garhwal Himalaya initiating over 50 small landslides within a study area of ~226 km^2 (Fig. 1). The earthquake was focused ~10.8 km WNW of Chamoli (30.49°N., 79.29°E.) at a depth of ~15 km

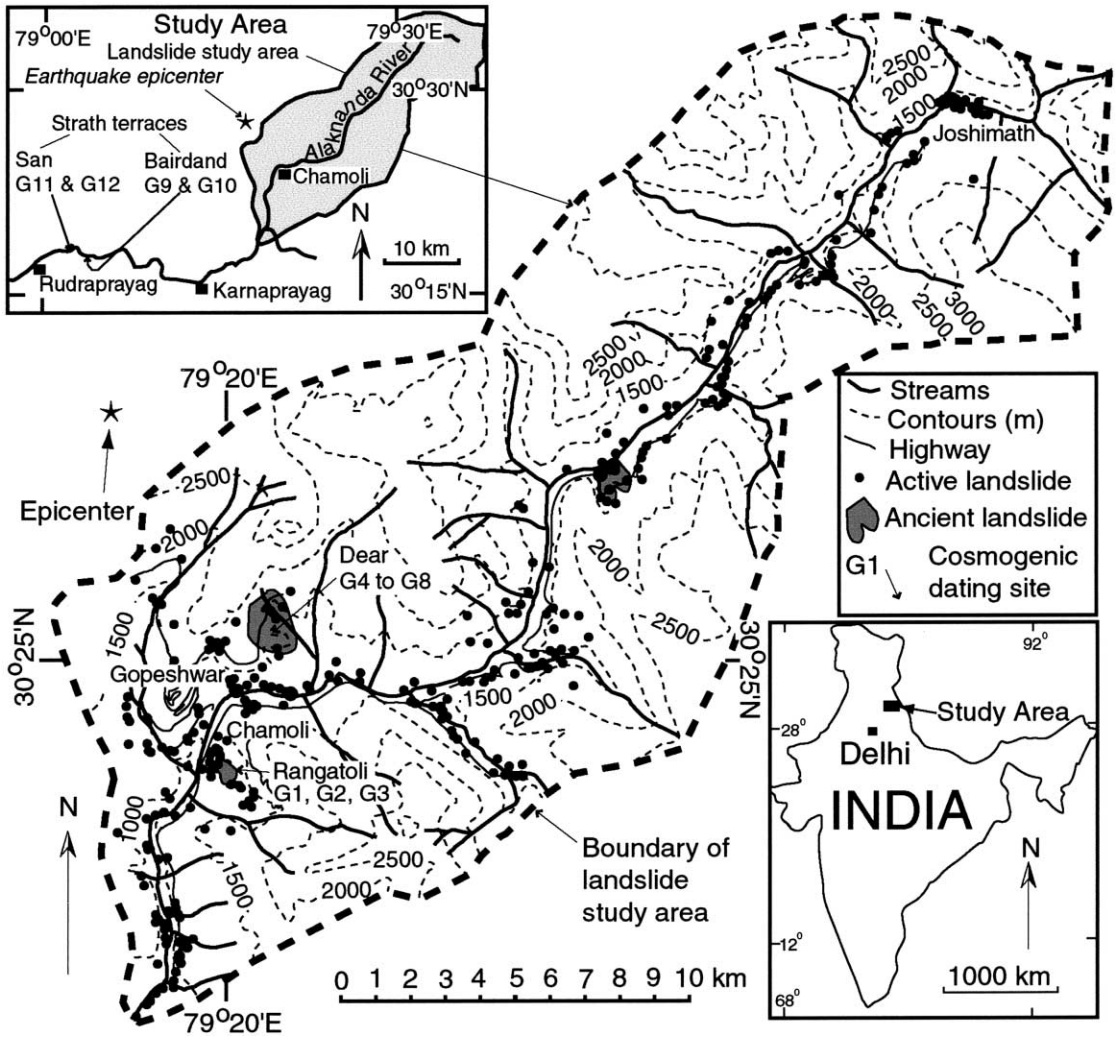

Fig. 1. The location of the study area and the distribution of active landslides. The location of the cosmogenic isotope dating sites is also shown. For clarity, each landslide is represented by a dot that is not to true scale.

(National Earthquake Information Service, 1999). This event, therefore, provided us with the opportunity to examine landslides that had been induced by natural processes, including earthquake shaking, and by human activity. It also allowed us to compare the effects of this quake with a similar study that was undertaken after the October 20, 1991, Garhwal earthquake ($M_b = 7.1$) that had an epicenter ~ 50 km NNW of the 1999 quake epicenter (Owen et al., 1995, 1996). This earlier earthquake resulted in ~ 700 fatalities and over 200 slope failures. Shortly after this earthquake and in the following monsoon season, Owen et al. (1995, 1996) mapped the distribution of earthquake- and rainfall-induced mass movements and measured the amount of debris involved in the mass movement events to calculate the equivalent landscape lowering during a large earthquake event and during the monsoon season. This 1991 study showed that the equivalent landscape lowering due to the earthquake- and rainfall-induced mass movements was ~ 0.007 and 0.02 mm, respectively. This was a surprising result because it suggested that mass movements might only be of minor importance in lowering Himalayan landscapes, based on the regional denudation rate of approximately several mm a^{-1} (Owen and Derbyshire, 1993; Burbank et al., 1996). The 1991 earthquake, however, was the only detailed study of the geomorphic effects of a large earthquake in the Himalaya and it may be atypical. Therefore, the 1999 earthquake also provided an opportunity to test the earlier results. It should be noted that the areas mapped in the two studies do not overlap, but comprise two different geographical regions, and therefore none of the landslides mapped in the 1999 study are associated with the 1991 study.

2. Geomorphic setting

The Garhwal Himalaya is located at the western end of the Central Himalaya in northern India (Fig. 1) and is situated in a seismic gap along the Main Central Thrust that separates the Lesser Himalaya to the south from the Greater Himalaya to the north (Valdiya, 1988; Metcalfe, 1993). This implies that seismic events are infrequent, but when they occur are commonly quite high in magnitude due to the build up of tectonic stress over time. The mountains rise to > 6000 m asl, while the valley floors drop to < 1000 m asl. The Bhagirathi and Alaknanda Rivers that flow into the Ganges drain the region. Fresh strath terraces (abandoned river channels in bedrock) several tens of meters above the river provide evidence of the rapid fluvial incision. Prior to the 1991 and 1999 earthquakes, the region experienced little seismic activity ($M > 6$) over the last 200 years (NOAA, 2000). The climate is monsoonal with heavy rainfalls mainly occurring in the summer, ~ 1500 mm a^{-1}, with typical monsoon showers dropping between 1 and 5 cm of rain per day (Indian Meteorological Department, 1989). Tropical weathering and mass movement produces thin regolith along the steep valley sides and is concentrated along the valley floors (Owen et al., 1996). Bedrock is commonly at a shallow depth (less than a few meters) or exposed and consists primarily of medium-grade metamorphic schist, gneiss, and quartzite with varying strikes and dips. Slides are common where bedrock dips approximate the valley side slope angle.

3. Methods

Four weeks after the Chamoli earthquake, an area of ~ 226 km^2 was studied in the region of the

Table 1
The main information recorded in the landslide inventory. A full database is available on compact disc upon request to the authors

(1) Landslide number; (2) Eastings; (3) Northings; (4) Altitude asl; (5) Landslide type; (6) Description of landslide; (7) Dimensions of failure scar; (8) Maximum angle of failed slope and direction; (9) Runout distance; (10) Type of runout; (11) Volume of accumulated debris; (12) Distance of debris from river/stream; (13) Distance of debris from settlements; (14) Distance of debris from highway/track; (15) Bedrock lithology; (16) Bedrock structure; (17) Regolith types and soil moisture; (18) Regolith thickness; (19) Vegetation type; (20) Percentage vegetation cover; (21) Stream types and slope drainage; (22) Stream density; (23) Human modification of slope; (24) Type of fissuring on slopes; (25) Length, width and depth of fissures; (26) Photographs of failure; (27) Additional comments.

epicenter (Fig. 1). Aerial photographs were not available because of political and logistical constraints, and satellite imagery was not used because it could not adequately resolve small failures. The accessibility to roads and trails and the region that could be directly observed from highways and trails delimited the boundary of the study area (Fig. 1). Every active slope failure with a slip face > 4 m^2 was located using a global positioning system and its location mapped on a 1:125,000 scale topographic map. An active slope failure was defined as one whose transported debris and failure scar were devoid of vegetation. Vegetation growth in this monsoon region is rapid, and therefore it is unlikely that the surface of an inactive landslide will remain free of vegetation for more than a few years to a decade (Schweinfurth, 1968; Rau, 1974; Singh and Singh, 1987). Earthquake-induced slope failures were identified by the evidence of very fresh debris on highways, trails of debris overlaying live vegetation, fresh failure scars

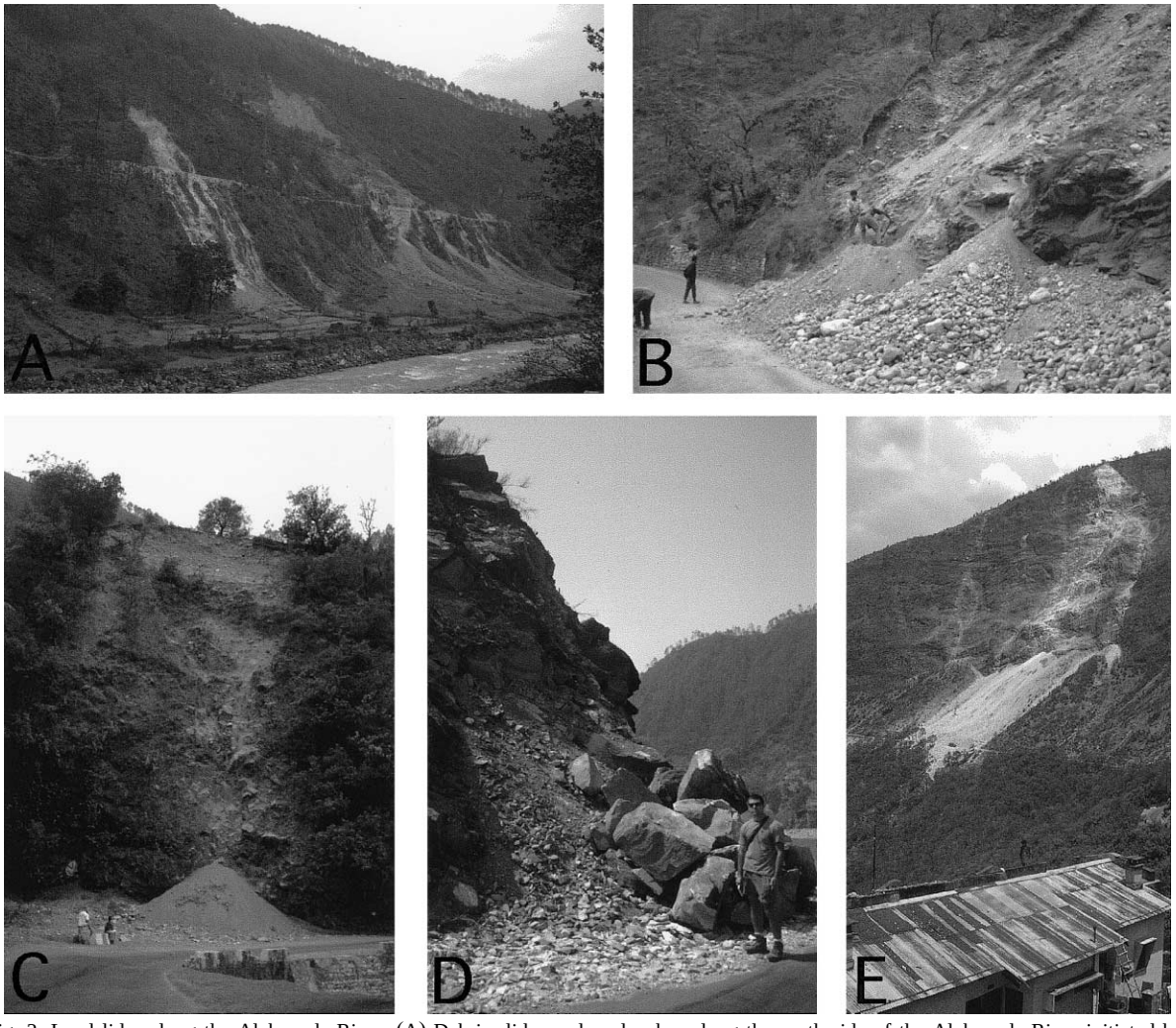

Fig. 2. Landslides along the Alaknanda River. (A) Debris slides and avalanches along the north side of the Alaknanda River initiated by highway construction (landslides #2 and #3; 79°19.2′E, 30°20.1′N). (B) Debris avalanches re-activated by the 1999 earthquake (landslide #23; 79°19.19′E, 30°21.15′N). (C) Debris avalanche initiated by highway construct and re-activated during the 1999 earthquake (landslide #105; 79°20.44′E, 30°24.26′N). (D) Debris avalanche initiated during the 1999 earthquake (landslide #130; 79°18.65′E, 30°29.16′N). (E) Debris avalanche partially re-activated during the 1999 earthquake (landslide #135; 79°19.1′E, 30°25.4′N).

Table 2
Types and numbers of active landslides and the equivalent landscape lowering

Type of failure	Number of failures	Number of failures affected by human activity	Total volume of material (m^3)	Net equivalent landscape lowering (mm)[a]	Percentage of total material involved/ equivalent landscape lowering
Earthquake-induced landslides					
Debris/rockfall	6	4	3452	0.015	0.27
Rock avalanche	14	9	2393	0.011	0.18
Debris avalanche	31	18	13 024	0.058	1.01
Debris flow	0	0	0	0	0
Debris/rock slide	5	4	1128	0.005	0.09
Total	56	35	19 997	0.089	1.54
Nonearthquake-induced active landslides					
Debris/rockfall	5	1	508	0.002	0.004
Rock avalanche	70	33	48 432	0.215	3.74
Debris avalanche	121	87	521 190	2.308	40.25
Debris flow	33	33	466 187	2.065	36.00
Debris/rock slide	53	39	215 158	0.953	16.62
Total	282	193	1 274 801	5.646	98.46
Earthquake- and nonearthquake-induced landslides					
Grand Total	338	228	1 294 797	5.735	100.00
Nonearthquake-induced landslides that showed evidence of remobilization during the earthquake[b]					
Total	248		186 278	0.825	14.39
Biggest landslides					
Top 3 (nonearthquake-induced landslides)	3		805 000	3.566	62.17
Top 10 (nonearthquake-induced landslides)	10		1 105 000	4.894	85.34
Top 30 (2 earthquake-induced landslides)	30		1 215 725	5.385	93.89

[a] The equivalent landscape lowering = total volume of material/study area (225.77 km^2).
[b] This volume of material and the net equivalent lowering is incorporated into the values shown in the nonearthquake-induced landslides.

that were free of dust and slope wash, and sometimes with the help of local people. All other failures were referred to as nonearthquake-induced landslides. Precipitation was virtually absent from the time of the earthquake until the study was completed, insuring that most fresh slides were a direct result of the earthquake. The characteristics of each failure were recorded on data sheets and photographed (Table 1).[1] The type of mass movement was identified using Varnes' (1978) classification, and the size of the failures was measured directly with a tape measure or surveyed using simple triangulation techniques. These data were incorporated into a database in a geographical information system.

Several large (> 0.5 km^2) ancient landslides were recognized in the region (Fig. 1). These were mapped, and samples from surface boulders were collected for cosmogenic radionuclide dating to help determine the age of two of the ancient landslides (Fig. 1). Samples for cosmogenic radionuclide dating were also collected from two of the strath terraces near Rudraprayag (Fig. 1). The height of the strath terraces above the present river level was determined by a survey using a tape measure and inclinometer. This allowed an independent measure of the rate of

[1] A full database and photographic record is available on compact disc upon request from the authors.

fluvial incision to be calculated for a comparison with the rate of denudation caused by landsliding.

The cosmogenic dating of rock samples was conducted at Lawrence Livermore National Laboratory by measuring ^{10}Be ($t_{1/2} = 1.5$ Ma) and ^{26}Al ($t_{1/2} = 0.705$ Ma) produced by cosmic rays in situ in the quartz crystals (Kohl and Nishiizumi, 1992). The samples were crushed and sieved to a uniform size of 250–500 μm. Approximately 90 g of this fraction was extracted and chemically leached to isolate the quartz per the methods of Kohl and Nishiizumi (1992), using HCl and HF:HNO_3 baths. Be carrier

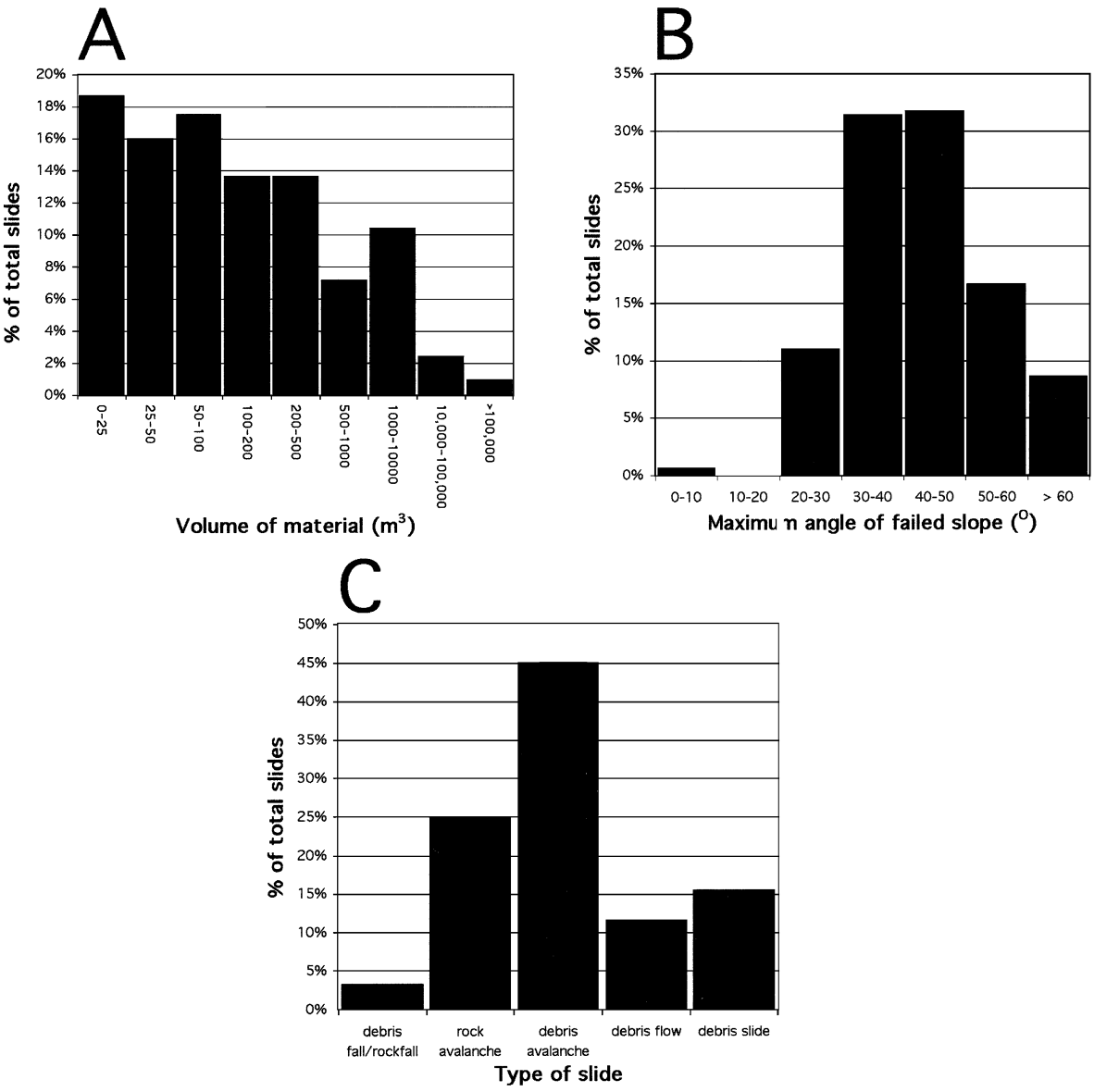

Fig. 3. Graphs summarizing key relationships of the landslide inventory showing the percent total landslides vs.: (A) volume of material; (B) maximum angle of failed slope; (C) type of slide; (D) regolith thickness; (E) runout distance; (F) type of failure material.

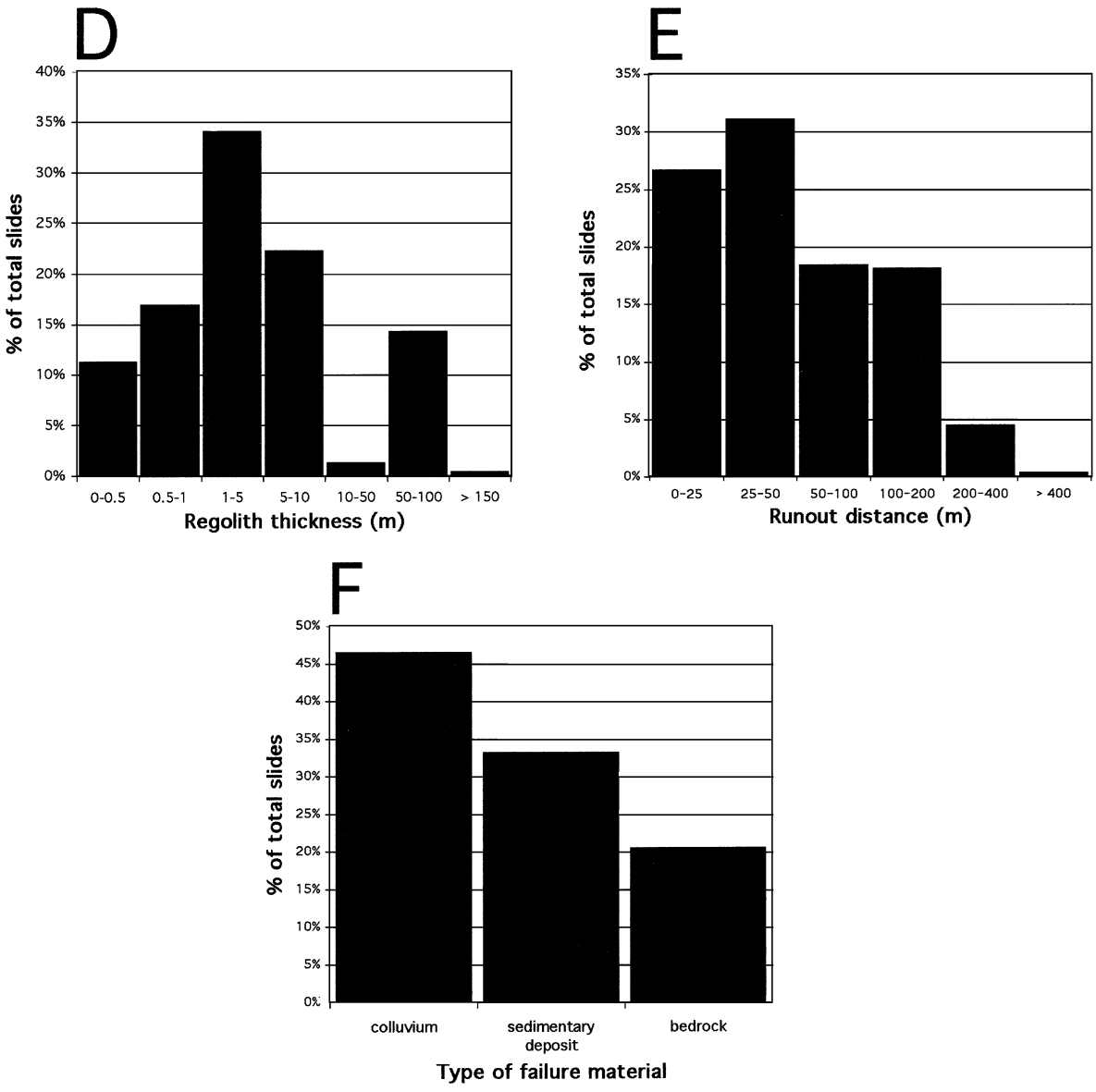

Fig. 3 (*continued*).

(0.5 mg) was added to the clean quartz separates, and the sample was then dissolved in 3:1 HF:HNO_3. An aliquot of the dissolved sample was used to determine the aluminum content using atomic absorption spectroscopy. Al and Be were separated in an ion exchange column. The processed samples were then loaded into the accelerator mass spectrometer to determine the ratio of the radionuclide to the stable isotope (Repka et al., 1997). Age determinations were based on the equations and production rates in Lal (1991) and Finkel and Suter (1993).

4. Results and discussion

Within the 226-km^2-study area, 338 active landslides were mapped, including 56 earthquake-induced landslides (Figs. 1 and 2). These comprised

mainly debris and rock avalanches (Table 2; Fig. 3). No debris flows were produced during the earthquake, although these were common among the non-earthquake-induced landslides. Rock avalanching was dominant in the higher elevations (>1500 m asl) where unconsolidated sediment was rare, although volumetrically their influence was insignificant. Debris flows, slides, and avalanches dominated the lower elevations. Undercutting of slopes by human activities such as road, footpath, or terrace construction, affected two-thirds of all recorded landslides (note the clustering of slides along the highways, Fig. 1). The overwhelming volume of mass movements occurred in the lower reaches (<1000 m asl) of the valleys in steep ($>30°$) metastable slopes. Only one-third of the landslides reached the streams, while another one-third of the landslides were >100 m away from any stream. Much of the landslide material was therefore temporarily stored on hill slopes that may be later reworked by creep and debris flow/slide processes. Unfortunately, there was no practical means to accurately date the residence time of this stored material, although the lack of vegetation in the majority of these areas hints at an extremely brief residence time. Nevertheless, the denudation rates stated in this paper are thus assumed to be the maximum possible because we have no means to quantify the exact rate as it would be impossible to determine the precise residence time of the stored material.

Most of the material moved was produced by a small number of landslides (Fig. 3; Table 2) and most landslides went to completion within a few days of the earthquake. Of the top 30 biggest slides (in terms of volume), only two were earthquake-induced (Table 2). The top 10 and top 3 biggest slides were all induced by rainfall events and accounted for over 85% and 62% of the volume of failed material, respectively. This supports the work of Brunsden and Jones (1984) in the Karakoram Mountains and Owen et al. (1996) in the Garhwal Himalaya, who showed that a small number of large failures are much more significant volumetrically than a large number of small failures.

The total volume of debris involved in active landsliding was ~ 1.3 million m^3 with only $\sim 1.5\%$ of this debris ($\sim 20{,}000$ m^3) moved during the quake within the study area. Keefer (1984) and Rodriguez et al. (1999) showed that earthquakes in their studies with a $M_s = 6.6$ could cause landsliding within an area of ~ 5000 km^2 and within a maximum distance of ~ 100 km from the epicenter. Since our study area was $\sim 5\%$ of the possible area where landsliding may have occurred, according to the work of Keefer (1984) and Rodriguez et al. (1999), then the total amount of landslide debris produced during the earthquake could approach ~ 0.4 million m^3 ($20 \times 20{,}000$ m^3). This is a maximum estimate because the study area stretched for about 30 km NE and 15 km S of the epicenter and should have experienced more landsliding than distant locations within the area that could possibly be affected by the earthquake, i.e., 100 km maximum distance from the epicenter. However, the variable geological conditions and type of earthquake are not taken into account by these studies in terms of their potential affect on the area of sliding. Earthquakes of comparable magnitude that have produced extensive landsliding have occurred in Arthur Pass, New Zealand in 1929 ($M_s = 6.9$; Adams, 1980), Mammoth Lake, California in 1980 ($M = 6.2$; Harp et al., 1984), Coalinga, California in 1983 ($M = 6.5$; Harp and Keefer, 1990), Loma Prieta, California in 1989 ($M = 7.0$; Keefer, 1998). These produced approximately 59, 12, 2, and 75 million m^3 of debris, respectively. Keefer (1994) presented an empirical study to provide upper limits on the amounts of debris that may be produced during earthquakes of different magnitudes. From this study, he suggested that the maximum volume of debris produced during a magnitude 6.6 earthquake was ~ 10 million m^3. The potential maximum volume of landslide material produced during the 1999 Garhwal earthquake is, therefore, small by comparison to other studies. This may be a result of the study area being located in an area where relatively resistant, medium-grade metamorphic rocks dominate the surficial geology, and situated along a steep river gorge where the potential sliding is reduced due to the lack of storage space for sediment on the steep valley walls. Notably, however, the number of studies including data on the volume of landslides produced are <20, and the Keefer (1994) empirical analysis only includes 15 studies. Therefore, it is difficult to assess whether the low volume of landslide debris that was produced in the Garhwal Himalaya is atypical of large earthquakes.

Table 3

(A) Cosmogenic isotope exposure ages for ancient landslides and strath terraces

Sample ID	Sample location	Shielding	Quartz wt. (g)	Be carrier wt. (mg)	Al ppm in qtz	Al carrier wt. (mg)	$^{10}Be/^{9}Be$ at/at (10^{-15})	^{10}Be (10^{6} atom/g)	$^{26}Al/^{27}Al$ atom/atom (10^{-15})	^{26}Al (10^{6} atom/g)	^{26}Al Exposure age (years)[a]	^{10}Be Exposure age (years)[a]	Average Exposure age (years)
Rangatoli landslide													
G1	30°23.319′N/79°20.030′E	0.995	15.087	0.4503	71.9	0.964	18.61 ± 1.76	0.0372 ± 0.0035	87.1 ± 6.5	0.2683 ± 0.0199	3427 ± 257	2860 ± 271	3158 ± 401
G2	30°23.314′N/79°20.011′E	0.994	15.104	0.4151	79.8	0.904	16.59 ± 1.50	0.0305 ± 0.0027	52.5 ± 6.3	0.1656 ± 0.0198	2107 ± 253	2339 ± 211	2244 ± 337
G3	30°23.317′N/79°19.954′E	0.985	15.096	0.4253	88.4	0.776	42.27 ± 3.07	0.0797 ± 0.0058	147.3 ± 12.2	0.4632 ± 0.0385	5975 ± 505	6188 ± 450	6094 ± 680
Dear landslide													
G4	30°25.337′N/79°20.811′E	0.997	25.446	0.4710	82.5	0.000	98.51 ± 3.02	0.1220 ± 0.0037	380.3 ± 24.0	0.6993 ± 0.0440	8035 ± 518	8431 ± 258	8352 ± 596
G5	30°25.337′N/79°20.811′E	0.987	25.433	0.4765	97.8	0.000	103.99 ± 3.60	0.1304 ± 0.0045	322.5 ± 14.6	0.7035 ± 0.0318	8083 ± 382	9011 ± 312	8640 ± 669
G6	30°25.327′N/79°20.854′E	0.997	25.617	0.5122	89.4	0.000	91.77 ± 2.86	0.1228 ± 0.0038	345.5 ± 16.6	0.6893 ± 0.0331	7946 ± 397	8515 ± 265	8339 ± 491
G7	30°25.735′N/79°20.895′E	0.993	25.163	0.5020	78.8	0.106	90.63 ± 3.57	0.1210 ± 0.0048	397.4 ± 22.8	0.7366 ± 0.0422	8241 ± 487	8138 ± 321	8169 ± 580
G8	30°25.710′N/79°20.919′E	0.993	24.956	0.5030	85.1	0.000	89.15 ± 3.64	0.1202 ± 0.0049	362.9 ± 19.2	0.6875 ± 0.0363	7690 ± 420	8087 ± 331	7935 ± 541
Bairdand strath terrace													
G9	30°17.802′N/79°03.487′E	0.978	20.080	0.4825	80.6	0.455	74.08 ± 2.28	0.1191 ± 0.0037	308.8 ± 12.2	0.7169 ± 0.0284	14976 ± 619	14991 ± 459	14986 ± 771
G10	30°17.802′N/79°03.487′E	0.978	25.205	0.4438	55.9	0.644	96.58 ± 2.86	0.1138 ± 0.0034	374.6 ± 30.5	0.6920 ± 0.0564	14452 ± 1195	14317 ± 421	14332 ± 1258
San strath terrace													
G11	30°18.339′N/79°02.973′E	0.997	25.133	0.4485	173.3	0.000	82.74 ± 3.15	0.0988 ± 0.0038	174.6 ± 9.7	0.6752 ± 0.0376	13848 ± 792	12207 ± 464	12627 ± 1291
G12	30°18.339′N/79°02.973′E	0.997	25.006	0.4560	131.8	0.000	108.10 ± 3.18	0.1319 ± 0.0039	269.7 ± 13.0	0.7931 ± 0.0384	16286 ± 81	16311 ± 479	16305 ± 946

(B) Calculations for incision rates

Sample ID	Strath terrace	Average exposure age (years)	Height above river (m)	Incision rate (mma^{-1})
G9	Bairdand	14986 ± 771	55	3.7
G10	Bairdand	14332 ± 1258	55	3.8
G11	San	12627 ± 1291	67	5.3
G12	San	16305 ± 946	67	4.1

[a]A Beryllium-10 ($t_{1/2}$ = 1.5 Ma) and ^{26}Al ($t_{1/2}$ = 0.705 Ma) concentrations were determined at the Lawrence Livermore National Laboratory Center for Accelerator Mass Spectrometry. Clean quartz was separated from these rocks by a chemical isolation method (Kohl and Nishiizumi, 1992). Beryllium-10 and ^{26}Al AMS measurements were carried out at the LLNL AMS facility. The observed ratios were normalized to ICN ^{10}Be and NIST ^{26}Al standards that were diluted by Nishiizumi (private communication, 1999). Minimum exposure ages and maximum erosion rates are calculated based on the production rates of ^{10}Be and ^{26}Al given in (Kohl and Nishiizumi, 1992) and on the latitude and elevation correction in (Lal, 1991) using geographic latitude. The appropriate values for sea-level high latitude production rates of ^{10}Be and ^{26}Al in quartz to be used in surface exposure dating studies are currently undergoing reassessment by a number of investigators. Pending resolution of this question, we have chosen to calculate minimum exposure ages based on the production rates of ^{10}Be and ^{26}Al given in Kohl and Nishiizumi (1992) and on the latitude and elevation correction in Lal (1991) using geographic latitude.

Given the volume of debris involved in the landsliding within the study area, active landsliding accounts for ~5.7 mm equivalent lowering of the landscape (volume of debris/study area) while the earthquake-induced failures account for ~0.09 mm of the net landscape lowering. Only two earthquakes of this magnitude have been recorded in the Garhwal Himalaya during the last 200 years, and if we, therefore, assume a ~100-year recurrence interval, then the average lowering per year by earthquake-induced landsliding would be ~0.009 mm. Individual landslides in this study region generally persist for periods of between ~1 and 10 years before they become vegetated and stable/metastable. Therefore, the net annual lowering of the landscape in the study area due to landsliding likely is in the order of 0.6–6 mm a^{-1} and is probably at the lower end of this range. Approximately two-thirds of these landslides

Fig. 4. Views of strath terraces along the Alaknanda River. (A) View looking West at the San strath terrace (30°17.8′N, 79°03.5′E) that is on the top of the rock bench on the right side of the plate. (B) The pot-holed surface of the San strath terrace. (C) View looking NE across the Bairdand strath terrace (30°18.3′N, 79°03′E).

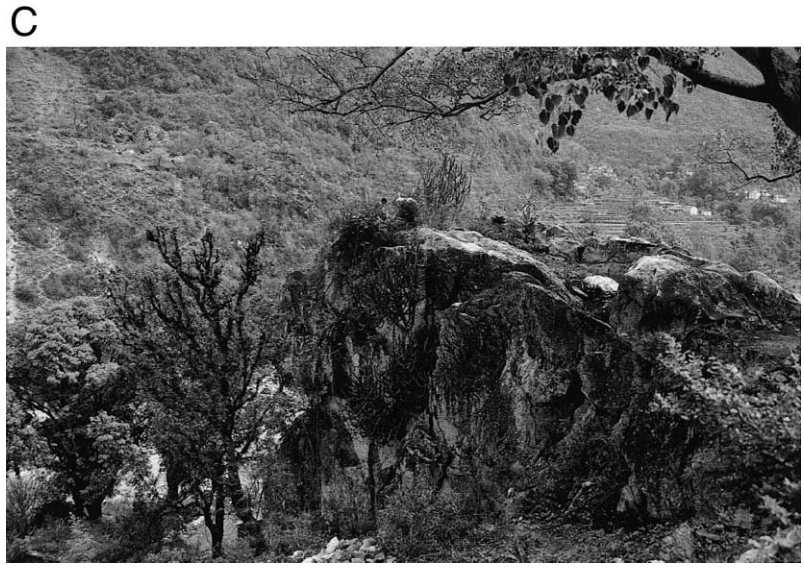

Fig. 4 (*continued*).

were initiated and/or aided by human activity (Table 2). This would thus further substantially reduce the natural net equivalent lowering of the landscape to between 0.2 and 2 mm a^{-1}. Granted, this extrapolation does not take into account the recurrence interval and magnitude of larger earthquakes, which may have a much greater impact on landsliding and denudation.

Denudation rates throughout the Himalaya are believed to be approximately several mm a^{-1} (Owen and Derbyshire, 1993; Burbank et al., 1996). Cosmogenic radionuclide dating of strath terraces near Rudraprayag show that the fluvial incision rate since the Late Glacial is ~ 4 mma^{-1} (Table 3; Fig. 4). Burbank et al. (1996) suggested that fluvial incision and hillslope mass wasting in the Himalaya are effectively coupled, and therefore fluvial valley lowering provides an estimate on the denudation rate for an individual catchment area. Therefore, the rate of denudation in the Alaknanda catchment area is likely to be ~ 4 mma^{-1}, equivalent to the fluvial incision rate calculated from dating the strath terraces near Rudraprayag. It may be argued that the strath terraces themselves could have been effectively lowered, but these are flat surfaces, and therefore the least prone to erosion, and thus provide an excellent dating site because erosion is minimal. Furthermore, the well-preserved water polished surfaces and relatively unweathered potholes testify to minimal erosion.

Therefore, a denudation rate of between 0.2 and 2 mm a^{-1} resulting from natural active landsliding, if the true value falls toward the upper end of the range, is an important component (5–50%) of the total denudation for this part of the Garhwal Himalaya. Furthermore, present-day denudation rates that include human-influenced landslides (~ 0.4–4 mm a^{-1}) approach the values for the average denudation rate throughout Late Glacial and Holocene times. This suggests that human activity is accelerating denudation within our study region.

In the 1991 study, Owen et al. (1996) estimated that the annual landscape lowering by rainfall- and earthquake-induced mass movements was ~ 0.02 mm and 0.000035 mm (0.007 mm/200-year earthquake recurrence interval), respectively. Clearly, the amount of landscape lowering by landsliding in the Chamoli region of the Garhwal Himalaya is at least an order of magnitude higher than in the area of the 1991 study. This difference is difficult to explain because both earthquakes had comparable characteristics and occurred during the dry season in similar geomorphic settings. During the previous study, the number of landslides may have been underestimated. This difference, however, more likely illustrates regional complexity and variability in the role of geo-

morphic processes throughout Himalayan environments; and in the area affected by the 1991 earthquake, less available sediment and less weathered rock may have been available. This may also be a function of the intensity of recent monsoon seasons that may have accelerated bedrock weathering, or the increased regolith thickness since the prior major event.

The largest landslides in the region are ancient and occur at three locations (Figs. 1, 5 and 6). They each comprise >10 million m^3 of stratified debris consisting of high (tens of meters) lobes of brecciated boulders. These characteristics are similar to those described in flow slides (sturzstroms) such as the Elm, Frank, and Blackhawk landslides (Heim, 1882; McConnell and Brock, 1904; Shreve, 1968). This suggests that these landslides occurred very rapidly and advanced at velocities >100 km h^{-1}. Cosmogenic radionuclide dating shows that two of these landslides occurred during the early and middle Holocene times (Table 3). The sturzstrom at Dear (Fig. 5; Table 3) yielded a much tighter cluster of dates (7.9–8.6 ka) as a result of the geomorphology of the slide (vertical slip face with a long (>1 km), flat run-out plain and a raised toe), its sedimentology (massive, with angular quartzite boulders in a pow-

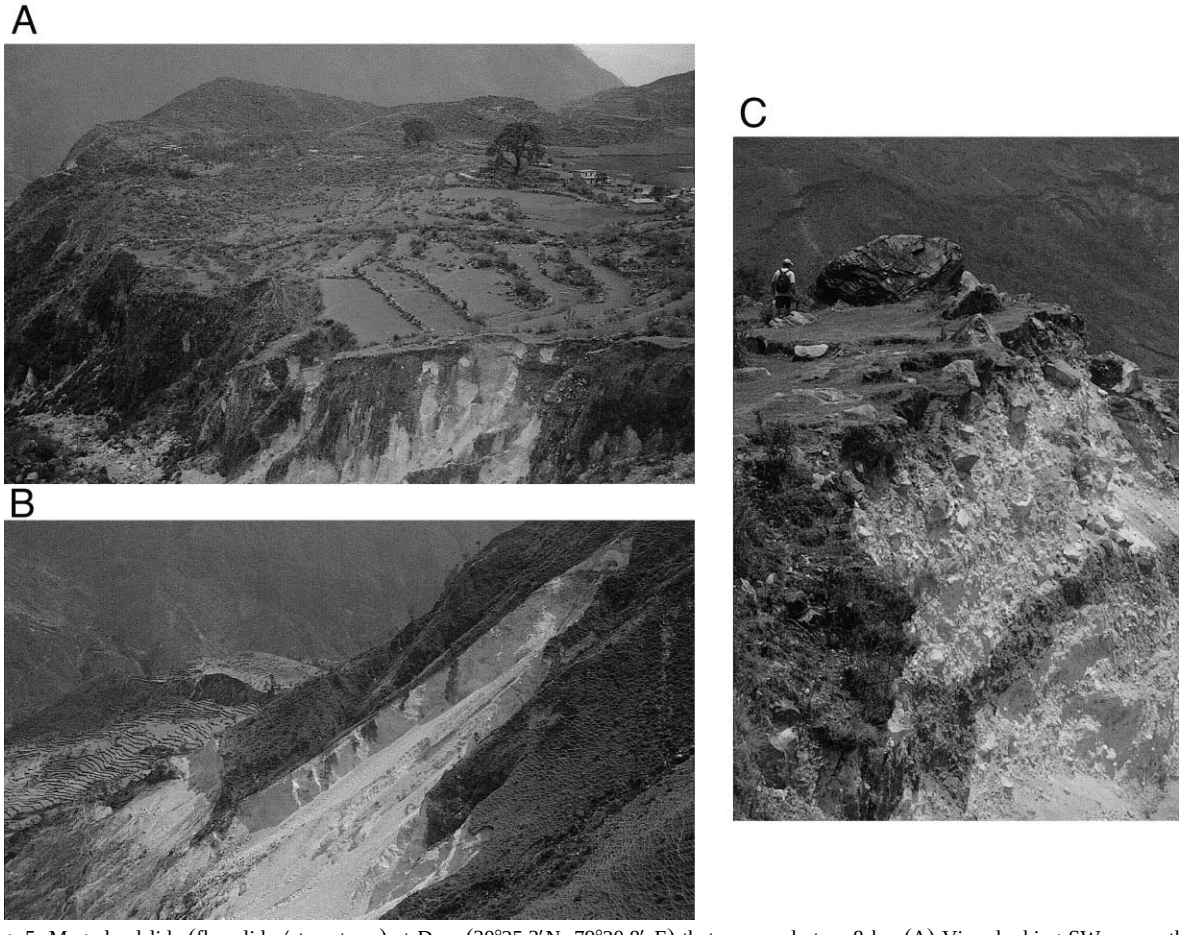

Fig. 5. Mega-landslide (flowslide/sturzstrom) at Dear (30°25.3′N, 79°20.8′ E) that occurred at $\sim$8 ka. (A) View looking SW across the southwestern end of the landslide deposit illustrating the frontal ridge and subsequent landsliding along its margin. The houses and terraces on the deposit provide a scale. (B) View looking SW at a recent landslide along the margin of the Dear mega-landslide. Most of this failure occurred during the rainfall events, but loose material was also mobilized during the 1999 earthquake. (C) View of part of the landslide debris illustrating how stratification has been preserved within the transported landslide debris.

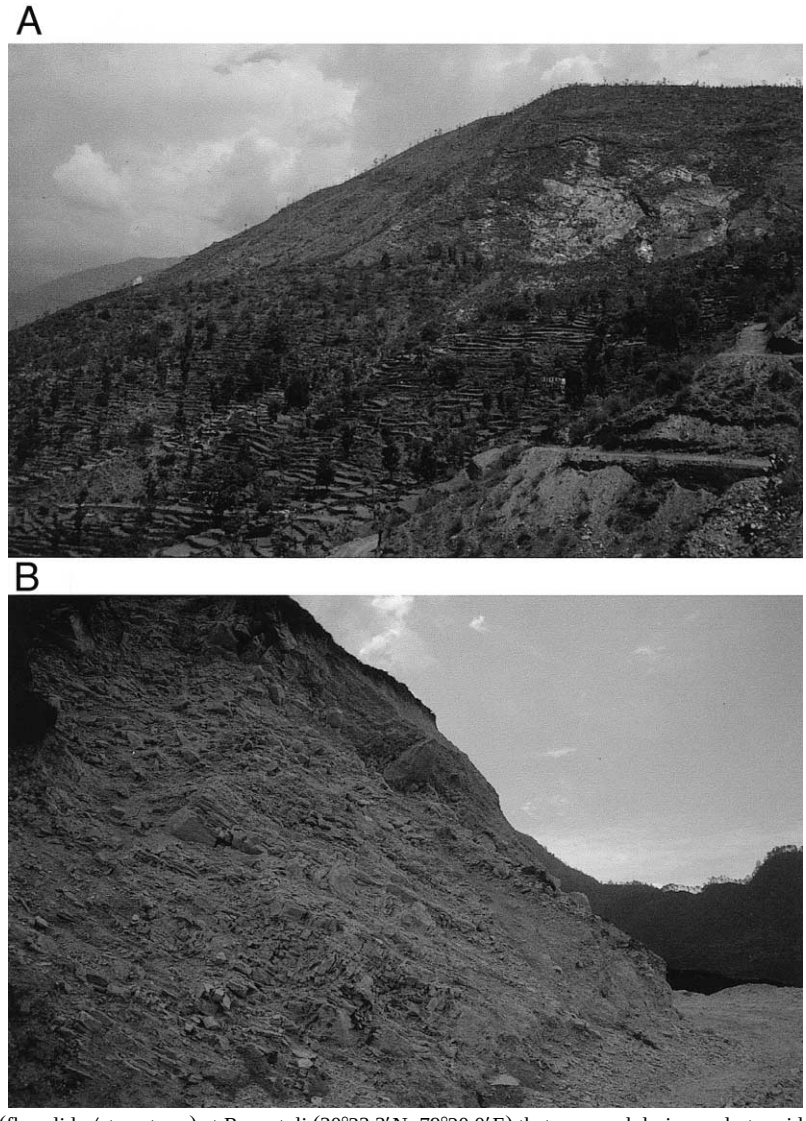

Fig. 6. Mega-landslide (flowslide/sturzstrom) at Rangatoli (30°23.3′N, 79°20.0′E) that occurred during early to middle Holocene times. (A) View looking NNE across the landslide, the whole of the terraced area in the middle of the plate comprises landslide debris and the scar on the hill slope in the distance is the part of the source for the landslide debris. (B) Excavation in the landslide debris showing the angular-blocking nature of the transported limestone.

dery sandy pebble matrix) and samples taken from boulders that protruded at the toe of the slide; collectively insuring that the entire deposit occurred as a single event, and none of the boulders sampled could have subsequently moved. The results show that dating a slide in this fashion can yield excellent results. The other sturzstrom sampled, at Rangatoli (Fig. 1; Table 3), was not nearly as ideal for dating as is evident by the wide range in dates it yielded (2.2–6.1 ka). Samples were taken from a small saddle in the center of a relatively steeply sloping run-out plain, and thus the potential for toppling and subsequent sliding was high, as the dating results illustrate. Problems of accessibility prevented sampling in a more ideal portion of this slide, but the results prove an important point in that great care

must be taken when interpreting the results of cosmogenic radionuclide dating when there is the potential for post-event movement. Determining whether earthquakes or changes in climate and/or hydrology initiated these landslides is not possible. Most of these landslides are still intact, and given that the duration of time since their failure is substantial then the actual amount of material removed from the mountains annually from these deposits is not very significant. They, therefore, contribute little to the net denudation of the mountains. However, they illustrate the importance of landslides as formative processes that produce new landforms and slopes that can persist in a Himalayan landscape for many millenniums.

Human activities have initiated and accelerated landsliding in this region primarily via the undercutting and removal of the toe of slopes for the cutting of roads and paths (note the cluster of failures mapped around roads, Fig. 1). This effectively removes a key component of the slope cohesion and strength and contributes to slope failure. Furthermore, this also serves to increase denudation rates, as failures along road or path cuts are commonly removed by discarding material on the downslope side of the failure. However, the precise contribution of human activities to regional denudation cannot be quantified.

This study and Owen et al.'s (1996) are limited geographically and temporally by logistical constraints. Care must, therefore, be taken when extrapolating rates of denudation throughout geological time and from small study areas to larger regions because the geology, topography, vegetation, and climate within the Himalaya are diverse. Local studies, however, are beginning to provide a database and raise questions as to the relative roles of earth surface and tectonic processes, and human activity in Himalayan environments. This study provides an estimate of the contribution of earthquake- and monsoon-induced landsliding for this region of Garhwal only, and direct comparisons to other studies can only be logically made where similar geologic and climatic conditions exist.

5. Conclusions

On the basis of cosmogenic radionuclide dating of strath terraces along the Alaknanda River, the natural rate of denudation in the study area within the Garhwal Himalaya since the Late Glacial is ~ 4 mm a^{-1}. Within the 226-km^2 study area, active landsliding has produced ~ 1.3 million m^3 of debris accounting for a lowering of the landscape of ~ 5.7 mm. Given that landslides generally persist for periods of between 1 and 10 years, landsliding accounts for an annual denudation of between ~ 0.6 and 6 mm. Human activity has influenced about two-thirds of the active landslides, and therefore human-influenced landsliding is helping to accelerate denudation in this part of the Himalaya. The volume of landslide material produced during the 1999 Garhwal earthquake ($\sim 20{,}000$ m^3) is relatively small compared to studies in other regions that experienced similar earthquakes. Although extrapolating denudation rates from a small area of the Himalaya to make regional generalizations is unwise, under similar geologic and geomorphic settings and climatic conditions, earthquakes of this magnitude are not very important in producing landslides that contribute to the gross denudation of the Garhwal Himalaya. However, natural landsliding that was not initiated by tectonic processes, for example, due to undercutting by streams and during heavy rainstorm events, are important in the gross denudation and as formative processes in shaping landscapes in this part of the Garhwal Himalaya.

Acknowledgements

To the people of Garhwal who lost more than 80 of their loved ones during the 1999 earthquake. This project was funded by a grant awarded to LAO from the National Science Foundation (EAR-9908403). Thanks to Kimberly Le who contributed to the data compilation and to Russell Campbell and David K. Keefer of the USGS for their helpful comments on an earlier version of this paper. We should also like to thank Professor R.A. Marston and two anonymous referees for their constructive comments on this paper. The cosmogenic radionuclide work was performed under the auspices of the U.S. Department of Energy by University of California Lawrence Livermore National Laboratory under contract No. W-7405-Eng-48.

References

Adams, J., 1980. Contemporary uplift and erosion of the Southern Alps, New Zealand. Geol. Soc. Am. Bull. 91, 1–114.

Brunsden, D., Jones, D.K.C., 1984. The geomorphology of high magnitude–low frequency events in the Karakoram Mountains. In: Miller, K. (Ed.), International Karakoram Project. Cambridge Univ. Press, Cambridge, MA, pp. 343–388.

Brunsden, D., Jones, D.K.C., Martin, R.P., Doornkamp, J.C., 1981. The geomorphic character of part of the Low Himalaya of eastern Nepal. Z. Geomorphol. 37, 25–72.

Burbank, D.W., Leland, J., Fielding, E., Anderson, R.S., Brozovic, N., Reid, M.R., Duncan, C., 1996. Bedrock incision, rock uplift and threshold hillslopes in the northwestern Himalayas. Nature 379, 505–510.

Finkel, R.C., Suter, M., 1993. AMS in the earth sciences: technique and applications. Adv. Anal. Geochem. 1, 114.

Gerrard, J., 1994. The landslide hazard in the Himalayas: geological control and human action. Geomorphology 10, 221–230.

Harp, E.L., Keefer, D.K., 1990. Landslides triggered by the earthquake. In: Rymer, M.J., Ellsworth, W.L. (Eds.), The Coalinga California Earthquake of May 2, 1983. U.S. Geol. Surv. Prof. Pap., vol. 1487, pp. 335–348.

Harp, E.L., Tanaka, K., Sarmiento, J., Keefer, D.K., 1984. Landslides from the May 25–27, 1980, Mammoth Lake, California, Earthquake Sequence. US Geological Survey Miscellaneous Investigation Series, Map I, 1612, scale 1:62,500.

Heim, A., 1882. Der Bergsturz von Elm: Zeitschrift der Deutschen. Geol. Ges. 34, 74–115.

Hewitt, K., 1998. Catastrophic landslides and their effects on the Upper Indus streams, Karakoram Himalaya, northern Pakistan. Geomorphology 26, 47–80.

Indian Meteorological Department, 1989. Climate of Uttar Pradesh. Government of India Publication, Delhi, pp. 372–375.

Ives, J.D., Messerli, B., 1989. The Himalayan Dilemma: Reconciling Development and Conservation. Routledge, London, 295 pp.

Keefer, D.K., 1984. Landslides caused by earthquakes. Geol. Soc. Am. Bull. 95, 406–421.

Keefer, D.K., 1994. The importance of earthquake-induced landslides to long-term slope erosion and slope-failure hazards in seismically active regions. Geomorphology 10, 265–284.

Keefer, D.K. (Ed.), 1998. The Loma Prieta, California, Earthquake of October 17, 1989-landslides. U.S. Geol. Surv. Prof. Pap., vol. 1551-C, 185 pp.

Kohl, C.P., Nishiizumi, K., 1992. Chemical isolation of quartz for measurement of in-situ-produced cosmogenic nuclides. Geochim. Cosmochim. Acta 56, 3583–3587.

Lal, D., 1991. Cosmic ray labeling of erosion surfaces: in situ nuclide production rates and erosion models. Earth Planet. Sci. Lett. 104, 429–439.

McConnell, R.G. and Brock, R.W., 1904. Report on the Great Landslide at Frank, Alberta, 1903. Department of the Interior, Government Printer. Ottawa, Dominion of Canada.

Metcalfe, R.P., 1993. Pressure, temperature and time constraints on metamorphism across the Main Central Thrust zone and High Himalayan Slab in the Garhwal Himalaya. In: Treloarand, P.J., Searle, M.P. (Eds.), Himalayan Tectonics. Geol. Soc. Spec. Publ., vol. 74, pp. 485–509.

National Earthquake Information Service, 1999. Preliminary Determination of Epicenters (PDE). Golden, Colorado.

NOAA, 2000. Significant earthquake database. http://www.ngdc.noaa.gov/seg/hazard/sig_srch.shtml.

Owen, L.A., 1991. Mass movement deposits in the Karakoram Mountain: their sedimentary characteristic, recognition and role in Karakoram landform evolution. Z. Geomorphol. 35 (4), 401–424.

Owen, L.A., Derbyshire, E., 1993. Quaternary and Holocene intermontane basin sedimentation in the Karakoram Mountains. In: Shroder, J.F (Ed.), Himalayas to the Sea: Geology, Geomorphology and the Quaternary. Routledge, London, pp. 108–131.

Owen, L.A., Benn, D.I., Derbyshire, E., Evans, D.J.A., Mitchell, W.A., Thompson, D., Richardson, S., Lloyd, M., Holden, C., 1995. The geomorphology and landscape evolution of the Lahul Himalaya, Northern India. Z. Geomorphol. 39, 145–174.

Owen, L.A., Sharma, M., Bigwood, R., 1996. Landscape modification and geomorphological consequences of the 20 October 1991 earthquake and the July–August 1992 monsoon in the Garhwal Himalaya. Z. Geomorphol. 103, 359–372.

Rau, M.A., 1974. Vegetation and phytogeography of the Himalaya. In: Mani, M.S. (Ed.), Ecology and Biogeography in India. W. Junk, The Hague, pp. 247–280.

Repka, J.L., Anderson, R.S., Finkel, R.C., 1997. Cosmogenic dating of fluvial terraces, Fremont River, Utah. Earth Planet. Sci. Lett. 182, 59–73.

Rodriguez, C.E., Bommer, J.J., Chanfler, R.J., 1999. Earthquake-induced landslides: 1980–1997. Soil Dyn. Earthquake Eng. 18, 325–346.

Schweinfurth, U., 1968. Vegetation of the Himalaya. In: Law, B.C. (Ed.), Mountains and Rivers of India. 21st International Geographical Congress, India, pp. 110–136.

Shreve, R.L., 1968. The Blackhawk Landslide. Geol. Soc. Am. Spec. Pap. 108, 47 pp.

Shroder, J.F., 1998. Slope failure and denudation in the western Himalaya. Geomorphology 26, 81–106.

Shroder, J.F., Bishop, M.P., 1998. Mass movements in the Himalaya: new insights and research directions. Geomorphology 26, 13–36.

Singh, J.S., Singh, S.P., 1987. Forest vegetation of the Himalaya. Bot. Rev. 53, 80–192.

Valdiya, K.S., 1988. Tectonics and evolution of the central sector of the Himalaya. Philos. Trans. R. Soc. London A 326, 151–175.

Varnes, D.J., 1978. Slope movements and types and processes. In: Eckel, E.B. (Ed.), Landslides: Analysis and Control. Special Report 176, Transport Research Board, National Academy of Science, Washington, D.C., pp. 11–33.